Eur. Phys. J. D **21**, 239–246 (2002)
DOI: 10.1140/epjd/e2002-00177-0

THE EUROPEAN PHYSICAL JOURNAL D

Electron dynamics in Na_9^+ and Pt_3 clusters from time-dependent Hartree-Fock theory

Y. Pavlyukh[1,a] and W. Hübner[1]

Max-Planck Institut für Mikrostrukturphysik, Weinberg 2, 06120 Halle, Germany

Received 28 March 2002 / Received in final form 31 May 2002
Published online 24 September 2002 – © EDP Sciences, Società Italiana di Fisica, Springer-Verlag 2002

Abstract. We present a method for the numerical investigation of the electron dynamics in small metallic clusters in intense laser fields. We obtain information about collective excitations and relaxation processes in the Na_9^+ and Pt_3 clusters analyzing the power spectrum of the dipole moment within a mean-field approach. The power spectrum is computed for various laser pulse parameters as well as for the limit of an infinitely short laser pulse. Due to the basis set expansion of the wave function our method is capable to follow the dynamics not only of the whole electron cloud, but of any particular molecular orbital.

PACS. 78.47.+p Time-resolved optical spectroscopies and other ultrafast optical measurements in condensed matter – 36.40.Cg Electronic and magnetic properties of clusters – 36.40.Gk Plasma and collective effects in clusters – 71.15.Ap Basis sets (plane-wave, APS, LCAO, etc.) and related methodology (scattering methods, ASA, linearized methods)

1 Introduction

During the recent years considerable progress has been achieved in the investigation of ultrafast electron dynamics in different systems: semiconductors, molecules and clusters, plasmas and magnetic materials [1–3]. At times shorter than the characteristic time of interaction, the dynamical behavior of the electrons cannot be described in terms of the relaxation time approximation, since scattering processes are not irreversible any more. This fact forms the essence of coherent control experiments and quantum computing, the general idea of which is switching the system from one quantum state to another by applying an external perturbation [4–6].

Lasers provide a unique excitation source for these purposes supplying pulses of an extraordinarily wide range of frequencies and intensities. Currently optical pulses as short as 10 fs or even less are available yielding a time resolution of about 1 fs. Typically experiments comprise the excitation of the system by a strong pump-pulse and the subsequent detection of the time evolution by monitoring its response to a second weaker pulse (probe) impinging after a variable time delay (so-called pump-probe experiments).

Besides electron-electron interaction, which is always the dominant relaxation process on the femtosecond time scale, there exists a variety of other relaxation mechanisms, depending on the system, such as: electron-phonon interaction, the role of which turned out to be very important in four-wave mixing experiments on semiconductors [7] and infrared photon echo study of liquids [8] or the generation of bulk and surface plasmons — collective plasma excitations. The latter seems to be significant for small metallic clusters and nanoparticles [9,10]. The possibility of experimentally investigating the electron dynamics in clusters [11] motivated us to develop a theoretical method, that is capable on the one hand correctly describe the energy level scheme and electron-electron interactions (this means the necessity to go beyond the semiclassical level of the Vlasov-LDA approach to the *quantum mechanical* description), and on the other hand to show this in a way closest to experiment, *i.e.* resolved in time.

Although all scattering mechanisms differ greatly with respect to the intensity, length scale and number of particles involved it is possible to classify them according to the relaxation time peculiar to each of the processes. Then at a given time stage one can pick up the dominating relaxation mechanism, neglecting other more slowly varying phenomena and build a correct approximation to the theory. In contrast to the single-particle picture, where changes of the quantum state can only be due to the interaction with an environment, the many-body nature of the electron gas also provides an internal clock mechanism. There exists a hierarchy of relaxation times corresponding to the equilibration of the one-, two-, three-particle distributions, etc. For each of the periods it is possible to build a quantum-kinetic theory [12,13] that takes into account the necessary number of correlation functions while neglecting correlation functions of higher order. The simplest approximation is to treat the electron dynamics on

[a] e-mail: pavlyukh@mpi-halle.de

the Hartree-Fock level, *i.e.* to neglect two-particle correlations.

The time-dependent Hartree-Fock equation is known for a long time since the early 1930s [14]. In the 1980s the formalism of time-dependent density functional theory [15] was established. Since that time, due to the development of enhanced computational equipment and efficient numerical algorithms, the solution of these equations was implemented for different systems such as particles in nuclear physics, clusters or plasmas using two different approaches: linear-response calculations [16,17] and full-fledged solution of the time-dependent problem [18,19]. The common feature of the latter approach is the real-space implementation. This means discretization of the space, as well as time axes. The advantages of this method are the possibility to study highly excited and unbound states, as well as the obvious interpretation of the results. On the other hand, static *ab initio* calculations in quantum chemistry are done, expanding all operators, the electronic density and wave functions in basis sets: Slater or Gaussian type. This treatment requires less computational effort, allows to study dynamics of any particular molecular orbital, describes electron transitions among states, which is impossible in the real-space methods, but is incapable of treating ionization processes [20].

In this paper we explain a numerical implementation of the time-dependent Hartree-Fock equation using a basis set expansion, show its advantage compared to the adiabatic and matrix-Hamiltonian treatment of the time-dependent problem. The method also has a more obvious interpretation of the solutions in terms of many-body perturbation technique than TDDFT theory, because for the limit of a weak deviation from the ground state analytical results are known.

In Section 2 we explain the numerical implementation of the method and the computation of the observables: the power spectrum of the dipole moment, the time-dependent populations of the molecular orbitals and the total energy. The power spectrum provides information about plasmon oscillations and excited states energies. In Section 3 we study collective effects in the Na_9^+ and Pt_3 clusters — systems with a larger number of the electrons, determine the energy, estimate the lifetime of the plasmon peak, and compare these results with other theoretical predictions and experimental data.

2 Theoretical background

The time evolution of the many-electron system can be reduced to the TDHF equation for the one-particle wave function $\psi(\mathbf{r},t)$:

$$\mathrm{i}\frac{\partial\psi(\mathbf{r},t)}{\partial t} = \Big[-\frac{1}{2}\Delta + \sum_{j=1}^{N}\frac{Z_j}{|\mathbf{r}-\mathbf{R}_j|} + \hat{H}_{\mathrm{d}}(\rho) + \hat{H}_{\mathrm{ex}}(\rho) + \hat{V}(t)\Big]\psi(\mathbf{r},t). \quad (1)$$

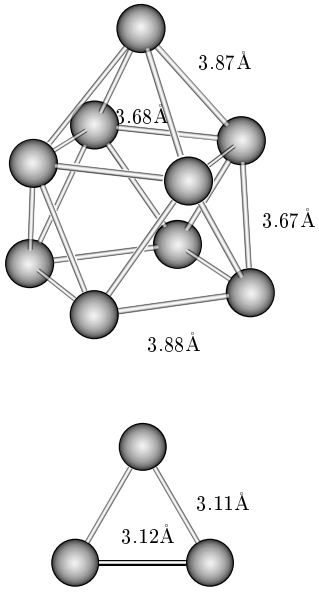

Fig. 1. Structures of Na_9^+ and Pt_3 clusters studied in this work. The numbers indicate the bond lengths in units of Å.

Note that the fundamental physical constants drop out by the use of atomic units. This equation describes the one-electron wave function $\psi(\mathbf{r},t)$ in the field of ions of charge Z_j at position $\mathbf{R}_j$. The interaction with other electrons is taken into account through the direct (H_{d}) and exchange (H_{ex}) energy functionals:

$$H_{\mathrm{d}}(\rho)\psi(\mathbf{r},t) = \int \mathrm{d}^3r' \frac{\rho(\mathbf{r}',\mathbf{r}',t)}{|\mathbf{r}-\mathbf{r}'|}\psi(\mathbf{r},t)$$

$$H_{\mathrm{ex}}(\rho)\psi(\mathbf{r},t) = -\int \mathrm{d}^3r' \frac{\rho(\mathbf{r},\mathbf{r}',t)}{|\mathbf{r}-\mathbf{r}'|}\psi(\mathbf{r}',t). \quad (2)$$

They depend self-consistently on the electronic density

$$\rho(\mathbf{r},\mathbf{r}',t) = \sum_{i=\mathrm{occupied}} \psi_i^*(\mathbf{r},t)\psi_i(\mathbf{r}',t). \quad (3)$$

We employ the Born-Oppenheimer approximation thus neglecting the motion of the atomic nuclei. In order to obtain information about the position of the nuclei $\mathbf{R}_j$ for the systems (Fig. 1) we have performed a geometry optimization on the Hartree-Fock level with the *Gaussian 98* package [21]. We take the perturbation operator $\hat{V}$ (interaction with laser field) in the most general form:

$$\hat{V}(t) = \mathbf{A}(t)\cdot\hat{\mathbf{p}} \quad (4)$$

as a scalar product of the vector potential of the electromagnetic wave $\mathbf{A}(t)$ and the electron momentum operator $\hat{\mathbf{p}}$. The temporal profile of the excitation source contains some slowly time varying envelope function multiplied by fast oscillations with the photon frequency.

This is more general than the commonly employed δ-pulses, because in this way we can not only study the response of the system to very short excitations, but also follow the dynamics *during* the pulse. Typically systems are excited by a laser pulse with temporal intensity distribution [11]

$$I(t) = I_0 \mathrm{sech}^2\left(\frac{t-t_0}{\sigma}\right). \tag{5}$$

The main quantity that distinguishes between regular and chaotic time evolution of the system and also gives information about excited states is the power spectrum of the dipole moment of the molecule. A detailed analysis of the properties of the power spectrum is given in reference [22]. The solution of the TDHF equation (1) yields the time evolution of the quantum states, from which we compute the time-dependent electron density (Eq. (3)) and subsequently — the expectation value of the dipole operator:

$$D_i(t) = \int \mathrm{d}^3 r\, r^L Y_{L,i}\left(\frac{\mathbf{r}}{r}\right)\rho(\mathbf{r},t) \tag{6}$$

with $L = 1$. The signal $D(t)$ is then Fourier transformed into the frequency domain, finally yielding the power spectrum:

$$P(\omega) = \int \mathrm{d}t \mathrm{e}^{\mathrm{i}\omega t} D(t). \tag{7}$$

Further observables are the populations of the molecular orbitals:

$$n_i(t) = \sum_{j=\text{occupied}} \langle \psi_i(\mathbf{r}, t=0) | \psi_j(\mathbf{r},t)\rangle \tag{8}$$

and the total energy of the system:

$$E(t) = \frac{1}{2}\sum_{i=\text{occupied}} \Bigg[\varepsilon_i(t) + \left\langle \psi_i(\mathbf{r},t)\right| -\frac{1}{2}\Delta + \sum_{j=1}^{N}\frac{Z_j}{|\mathbf{r}-\mathbf{R}_j|} + \hat{V}(t)\left|\psi_i(\mathbf{r},t)\right\rangle\Bigg] \tag{9}$$

where $\varepsilon_i(t)$ are the instantaneous eigenvalues of the Hamiltonian. Using a basis set expansion of the wave functions makes the computation of these quantities a trivial task as the space integration in the above formulas simply reduces to the computation of the scalar product of two vectors.

The general scheme for solving equation (1) is as follows: initially, we perform a stationary self-consistent field (SCF) calculation in order to obtain the wave function of the ground state. Then we use this as the initial condition for the system of ordinary differential equations to which equation (1) reduces after expanding all operators and functions in a given basis set. We propagate the solution in time by an adaptive Runge-Kutta or Bulirsch-Stoer method [23]. The elementary time step, which strongly depends on the system, is of the order of 10^{-3} fs. Thus, typically 10^6 steps are needed in order to obtain the solution for 200 fs. It is instructive to compare the performance of our method with the standard version of the real space TDLDA [19]. In the latter case the number of mesh points must be taken much larger than the number of basis functions in our implementation in order to correctly reproduce the electronic structure with the same accuracy (27 609 points for the Na_{147} cluster compared to 72 (upscaling to 1 176 in the case of Na_{147}) basis functions for our Na_9^+ cluster). The number of integration steps in the case of TDLDA for the Na_{147} is reduced to only 5 000 using integrators with fixed step-size in reference [19].

The most time consuming computational step — the evaluation of the matrix elements of the direct and exchange energy functionals (Eq. (2)) could be done efficiently, using Raffenetti's [24] format for the electron repulsion integrals (ERIs)

$$\langle \alpha\beta|\gamma\delta\rangle = \int \mathrm{d}^3 r \mathrm{d}^3 r' \frac{\phi_\alpha(r)\phi_\beta(r)\phi_\gamma(r')\phi_\delta(r')}{|\mathbf{r}-\mathbf{r}'|} \tag{10}$$

$$\alpha,\beta,\gamma,\delta = 1...N_{\mathrm{bf}}. \tag{11}$$

N_{bf} is the number of basis functions $\phi_{\alpha,\beta,\gamma,\delta}$, which is proportional to the number of atoms in the system and the number of electrons. For the closed-shell calculation one has:

$$\begin{aligned} H_{\mathrm{d-ex}} &= H_{\mathrm{d}} + H_{\mathrm{ex}} \\ \mathrm{Re}({\mathrm{H_{d-ex}}}^{\alpha\beta}) &= \sum_{\substack{\gamma\delta \\ \gamma>\delta}} I_{\alpha\beta,\gamma\delta}\mathrm{Re}(D_{\gamma\delta}) \\ \mathrm{Im}(H^{\alpha\beta}_{\mathrm{d-ex}}) &= \sum_{\substack{\gamma\delta \\ \gamma>\delta}} J_{\alpha\beta,\gamma\delta}\mathrm{Im}(D_{\gamma\delta}) \end{aligned} \tag{12}$$

$$\begin{aligned} I_{\alpha\beta,\gamma\delta} &= 2\langle\alpha\beta|\gamma\delta\rangle - 0.5(\langle\alpha\gamma|\beta\delta\rangle + \langle\alpha\delta|\beta\gamma\rangle) \\ J_{\alpha\beta,\gamma\delta} &= -0.5(\langle\alpha\gamma|\beta\delta\rangle - \langle\alpha\delta|\beta\gamma\rangle) \end{aligned}$$

where the $\langle\alpha\beta|\gamma\delta\rangle$ are the ERIs and the $D_{\alpha\beta}$ are the matrix elements of electronic density (Eq. (3)):

$$\rho(\mathbf{r},\mathbf{r}',t) = \sum_{\alpha,\beta} D_{\alpha\beta}(t)\phi_\alpha(\mathbf{r})\phi_\beta(\mathbf{r}'). \tag{13}$$

Then the computation of the Hamiltonian matrix elements can be reduced to simple matrix-vector operations, that can be implemented very efficiently. In this case, for the closed-shell system, the numerical cost of the method scales as

$$N_{\mathrm{op}} = 2N_{\mathrm{t}}(N_{\mathrm{bf}}(N_{\mathrm{bf}}+1)/2)^2 \tag{14}$$

and for the open shell system it is approximately 1.5 times larger. N_{t} is the number of time steps. From the numerical point of view it is better to propagate only the wave functions of the initially occupied states, rather than the full density matrix (Eq. (3)).

For clusters with a large number of electrons the optimum choice of basis functions matters a lot, on the one

hand restricting the precision of the wave function representation and on the other hand limiting the maximum number of time steps. In order to obtain solutions for the longest possible time intervals, and thus, to get a high resolution for the Fourier transformed quantities we use an effective core potential (ECP) together with lanl2dz basis set for the Na_9^+ and Pt_3 clusters (Dunning-Huzinaga full double zeta on the first row [25], Los Alamos ECP plus DZ on Na-Bi [26]).

In the limit of linear response, *i.e.* when perturbations are small, the TDHF equation could be linearized, and thus reduces to the eigenvalue problem. For a long time, linearized time-dependent Hartree-Fock (LTDHF) or DFT methods have been the only possibilities to study excitations in the realistic quantum systems on the *ab initio* level (for a review on early applications of these methods to metallic clusters see Brack, reference [27], and the references [16,17] for the thorough comparison of the different types of TDDFT linear response calculations, that can be viewed as a low-fluence regime of the problem). Detailed information about the system, *i.e.* excitation energies, plasmon dispersion, or polarizability, could be obtained assuming a small deviation of the wave functions from the stationary state. For the uniform electron gas, results obtained in that way coincide with the diagrammatic calculation within the random phase approximation (RPA) [28]. The Lindhard dielectric function is obtained from the RPA expression assuming an equilibrium electron distribution. In the case of finite temperature or an electron distribution away from equilibrium (*which was studied in our case*) the dielectric function must be evaluated in the whole complex plane. The plasmon frequency and decay can then be found at the intersection of the $\mathrm{Re}(\epsilon) = 0$ and $\mathrm{Im}(\epsilon) = 0$ curves [29]. In our case we study a situation close to the experiment (such as described in Ref. [11]). The laser pulse interacts with the cluster and part of the photon energy is absorbed. The electron distribution becomes different from a step function and can be approximately treated introducing an effective non-zero temperature. Thus, the analogy to the RPA result, as well as recent results on the plasmon dispersion from the adiabatic LDA [30] support our expectations, that a full-fledged time-dependent treatment will yield reliable information about one-particle and collective excitations, plasmon life-times in metallic clusters, which, on the other hand are experimentally accessible.

To better understand the general behavior of the solutions of TDHF, we compare the anticipated dynamics from this method with other one-particle methods for the investigation of the time evolution of quantum systems (see Fig. 2). In the TDHF scheme, shortly after the system has been excited it exhibits oscillations with the plasmon frequency (Fig. 2c), which is the zero of the longitudinal dielectric function on the RPA level. For the electron gas the dielectric function is given by the Lindhard formula, and already on the LTDHF level it possesses an imaginary part, *i.e.* this means a decay of the plasmon oscillation in time. But, as scattering processes are not very accurately described in the mean field approximation, the plasmon oscillation will last considerably longer in time, compared to the higher level treatment of electronic correlations (Fig. 2d). In the regime of a slowly varying external field we can expect the adiabatic approximation to give a reasonable result. In that way, instead of solving equation (1) we self-consistently solve the quasistationary eigenvalue problem:

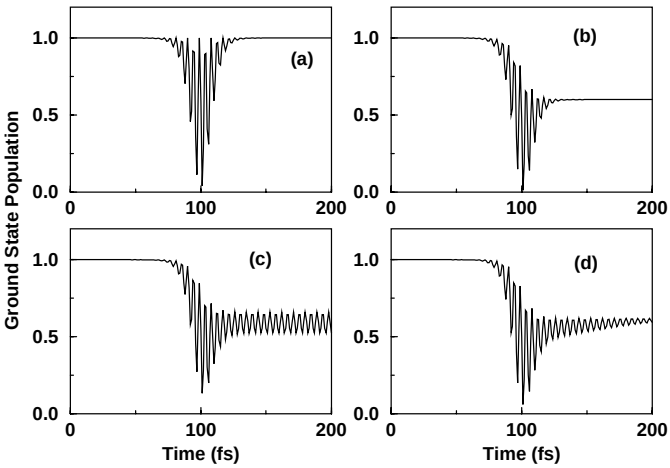

Fig. 2. Anticipated typical time evolution of the electron population within different approaches. (a) Adiabatic solution of Hartree-Fock equation. (b) Evolution of matrix Hamiltonian, Rabi oscillations. (c) Solution of the TDHF equation. (d) Full quantum kinetic solution.

$$[\hat{H}_{HF}(\rho) + \hat{V}(t)]\psi(\mathbf{r},t) = E(t)\psi(\mathbf{r},t), \tag{15}$$

which provides the instantaneous eigenvalues and eigenstates. The main feature of this approach is that it is fully reversible, and, after switching off the perturbation, the systems returns to its initial state (Fig. 2a).

Another approach to study the time evolution is to find excitation levels of the system, which in the many-body picture do not coincide with the quasiparticle states of the Hamiltonian and should be determined on a higher level, *e.g.* by the CI method or as the poles of the two-particle Green function. Then we can follow the electron dynamics of the system in the basis of ground and excited states. The Hamiltonian in that case could be represented in a matrix form, with energies of the ground ε_0 and excited $\varepsilon_1, ..., \varepsilon_n$ states on the diagonal, and off-diagonal matrix elements of the perturbation operator:

$$\begin{pmatrix} \varepsilon_0 & V_{01} & \cdots & V_{0n} \\ V_{10} & \varepsilon_1 & \cdots & V_{1n} \\ & & \ddots & \\ V_{n0} & V_{n1} & \cdots & \varepsilon_n \end{pmatrix} \begin{pmatrix} \psi_0(\mathbf{r},t) \\ \psi_1(\mathbf{r},t) \\ \vdots \\ \psi_n(\mathbf{r},t) \end{pmatrix} = \mathrm{i}\frac{\partial}{\partial t} \begin{pmatrix} \psi_0(\mathbf{r},t) \\ \psi_1(\mathbf{r},t) \\ \vdots \\ \psi_n(\mathbf{r},t) \end{pmatrix}. \tag{16}$$

Here the matrix elements of perturbation operator correspond to the transitions between different states:

$$V_{i,j}(t) = \langle \psi_i(\mathbf{r}) | V(\mathbf{r},t) | \psi_j(\mathbf{r}) \rangle. \tag{17}$$

The evolution of such a system has widely been studied in the literature [31], but even in the simplest case of a

Table 1. Parameters of the time-dependent calculation. As all systems are closed-shell N_e means the number of electron pairs. N_{ECP} is the number of electrons replaced by the effective core potential.

System	Fig.	N_{bf}	N_e	I_0 $[10^{11}\mathrm{W/m^2}]$	N_{ECP}	basis set Ref.
Na_9^+	3	72	4	107.6	10	[25]
Pt	4	72	24	2.1	30	[26]
Pt	5	72	24	1.4–2.8	30	[26]
Pt	6	15–25	5–10	0.0	30	[26]

two level system this equation has no analytical solution. In the rotating wave approximation (RWA) we have so called Rabi oscillations [32] between levels, which accompany transitions from one to another state. After termination of the external perturbation the system displays no more oscillation, but, in contrast to the adiabatic approximation it remains in the last state it achieved. This state could be different from the initial state, and, if no further perturbation takes place, the system will remain in that state forever (Fig. 2b). The evolutions of the quantum system of the types (a), (b) and (c) although based on the different approaches for the treatment of the time dependence can be accessed on our level of theory by properly defining the Hamiltonian matrix elements (with self-consistent dependence on the density in cases (a) and (c), or without self-consistency in case (b)). The case (d), which is shown for the comparison describes the ideal situation, when the chain of quantum kinetic equations is not broken at a certain level. From these considerations we can see, that the time-dependent Hartree-Fock equation is capable of explaining the gross features of the quantum evolution of the system, such as reversibility *vs.* irreversibily, transitions between states, plasmon oscillations, which cannot be achieved in the simpler theories. This approach has also the option of a systematic improvement through the replacement of the exchange energy by the exchange-correlation functional from the DFT.

3 Power spectra of metal clusters

In simple systems, such as Na_4, the electronic density of states is small. This leads to a power spectrum with well separated peaks that correspond to one particle-hole ($1ph$) excitations. Considering more complicated systems such as Na_9^+ and Pt_3 (see Tab. 1 for the information about the number of basis functions, electrons in the active space and laser pulse parameters), with a larger number of electrons, a new feature in their power spectra can be observed. Because of the dense level scheme in these clusters many $1ph$ states merge and form a collective excitation — a plasmon — due to their constructive interference. In contrast to one-particle excitations, the oscillator strength of the plasmon is very high and it manifests itself as a strong peak in the power spectrum of the dipole moment.

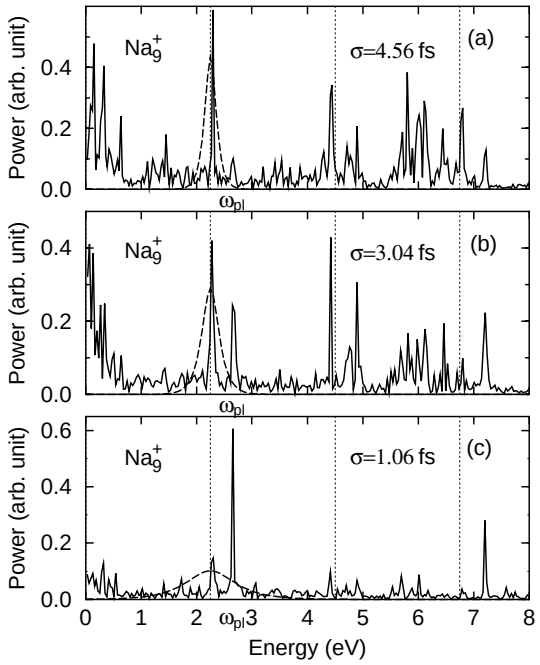

Fig. 3. Power spectra of the Na_9^+ cluster, excited with laser pulses of the same photon energy and different pulse width. Dashed line shows the Fourier transform of the pulses of different duration: (a) $\sigma = 4.56$ fs, (b) $\sigma = 3.04$ fs, (c) $\sigma = 1.06$ fs. Vertical lines denote energies, that correspond to the one-, two- and three-photon processes.

In contrast to the response function, which only characterizes the internal properties of the system, such as the energies and the oscillator strengths of the excited states, the power spectrum depends as well on the parameters of the external excitation. To study intrinsic properties of the system one has to minimize the role of the second factor. This can be done by putting the system initially in some nonequilibrium state and then following its relaxation [22] or one uses very short pulses, that embrace a large frequency interval.

We performed a series of calculations on Na_9^+ cluster for pulses of the mean photon frequency $\omega^* = 2.25$ eV and different durations (Fig. 3). The polarization of the electric field is taken to be along the axis of axial symmetry of the cluster. When the frequency width of the pulse is small predominantly states that correspond to the absorption of one, two, and three photons (denoted by vertical lines) are well pronounced. The plasmon peak at 2.7 eV is almost invisible (see Fig. 3a). Shorter pulses lead to a broader region of energies in which absorption can take place and thus excitations of the states that are further away from the resonance, but of higher oscillator strength become possible. Our value for the position of the plasmon peak, determined as a excitation with the highest oscillator strength that can be excited off-resonantly (Fig. 3c) ($\omega_{pl} = 2.7$ eV) of the Na_9^+ cluster is in good agreement with results obtained within the real-space implementation of TDLDA (Refs. [22,33–36]). In spite of this its oscillator strength is considerably lower in our approach.

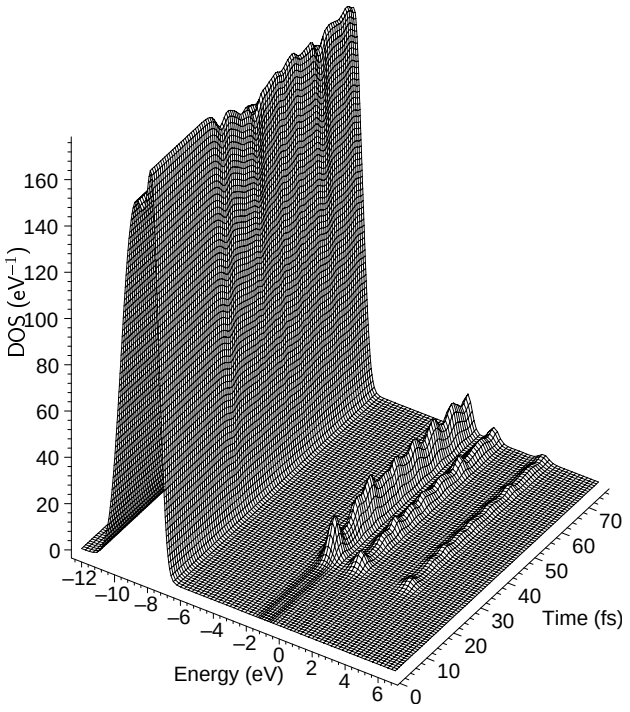

Fig. 4. Time-resolved density of states of the Pt_3 cluster, excited by a laser pulse with $\omega^* = 3.125$ eV. Gaussian broadening of width 0.27 eV has been used.

We think that this may be caused by the difference in the excitation mechanisms used (initial dipole shift of the entire electron cloud *vs.* excitation with certain frequency and time profile) and the number of electrons, taken into account. The plasmon, as a collective effect is very sensitive to the density of virtual states in the system. Replacing part of the inner electrons with an effective potential may have small impact on the ground state properties, but may imply a sophisticated analysis in the case of excited states.

To better understand the possibility of the non resonant plasmon excitation and in order to estimate the plasmon lifetime we apply our technique to the previously experimentally studied cluster Pt_3 (Eberhardt and coworkers, [11]). It has been shown that the cluster possesses a very dense metallic like energy-level structure [37], leading to the enhancement of electron-electron scattering processes. The latter causes an effective energy transfer from one $1ph$ state to another, thus considerably reducing the plasmon lifetime in open-shell transition metal clusters compared to noble or alkali metal clusters. In calculations we use pulses of the same duration $\sigma = 0.76$ fs and different photon energy in a range from $\omega^* = 2.625$ eV to $\omega^* = 3.625$ eV that is in either case below the plasmon energy (Fig. 5). Polarization of the electric field is perpendicular to the plane of Pt_3 cluster. A typical time evolution of the density of occupied states, computed as

$$\rho(\epsilon, t) = \sum_i n_i(t)\delta(\epsilon - \varepsilon_i) \tag{18}$$

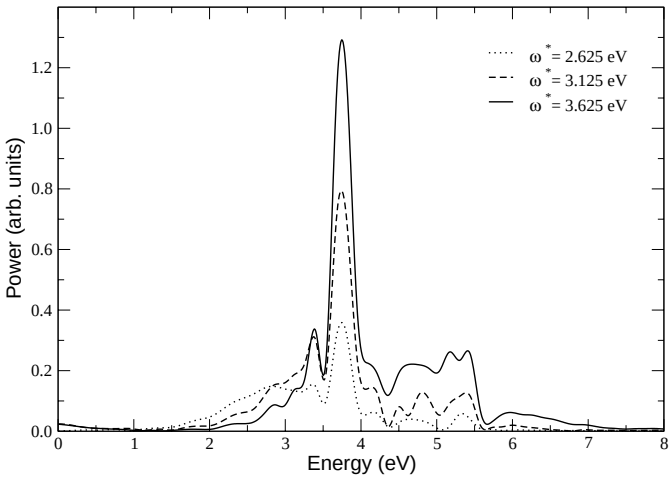

Fig. 5. Power spectra of the Pt_3 cluster, excited with laser pulses of the same width and different photon energies: dotted line — $\omega^* = 2.625$ eV; dashed line — $\omega^* = 3.125$ eV; solid line — $\omega^* = 3.625$ eV.

is shown in Figure 4 ($n_i(t)$ is computed according to Eq. (8)). A transition of the part of electronic population from the occupied states close to Fermi level to previously unoccupied states occurs shortly after applying the laser pulse and leads to complicated oscillations.

The use of very short pulses, although at present experimentally not feasible allows us to cover a very large energy range and to study fast processes far from resonance.

One can see (Fig. 5) redistribution of the spectral weight of the peaks with the change of excitation energy. The magnitude of the plasmon peak strongly depends on the vicinity of the photon frequency to the plasmon pole. The spectral weight of the shoulder in the region of energies 2–3.5 eV decreases when ω^* approaches the plasmon resonance at $\omega_{\rm pl} = 3.7$ eV.

As mentioned above, the plasmon is a collective effect that originates from the strong enhancement of the one-particle excitations due to the constructive interference [22,38]. If a time-dependent calculation is performed on very long time scales, it would be possible to resolve plasmon peak as a very dense structure of individual $1ph$ peaks of very small width. In the higher order correlation treatment these peaks will be smeared out to form one envelope that will resemble the plasmon peak at the present level of the theory (for the discussion of plasmon width as a result of fragmentation of the resonance into nearby $1ph$ states and comparison with another mechanism — broadening due to the thermal fluctuations see Ref. [39]). That is why it is natural to use information from mean-field calculations in order to extract information about plasmon lifetime. The plasmon peak can be viewed as a Lorentzian or Gaussian peak. The first case describes a $e^{-\frac{t}{\tau}}$ decay of the quasiparticle in the many-body system, while the second one corresponds to the inhomogeneous broadening of the peak. The decay law is then $e^{-\frac{t^2}{\tau^2}}$. The lifetime can differ up to a factor of 2π depending on the choice of the

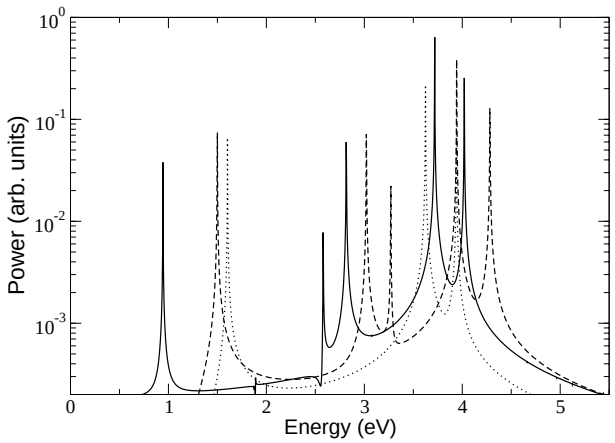

Fig. 6. Power spectra of the Pt_3 cluster, for different numbers of electrons and basis functions: dotted line — $N_e = 5$, $N_{bf} = 15$; dashed line — $N_e = 10$, $N_{bf} = 20$; solid line — $N_e = 10$, $N_{bf} = 25$.

model. We perform a non-linear fitting of the power spectrum by a set of Lorentzians (a similar idea can be found in the recent work of Molina *et al.*, Ref. [40]):

$$P(\omega) = \sum_i \frac{A_i}{2\pi} \frac{\delta_i}{(\omega - \omega_i)^2 + \delta_i^2} \tag{19}$$

and find the width of the plasmon peak to be $\delta_{pl} = 0.17$ eV that corresponds to a lifetime of approximately $\tau_{pl} = 24$ fs ($\tau_{pl} = 3.8$ fs in the case of a Gaussian model). This result should be compared with experimental data of Eberhardt and coworkers [11], who determined the lifetime to be less than 70 fs and attributed it solely to electron-electron scattering.

Up to now we were interested only in the properties of the system, excited in the way similar to the experiment. For comparison the *clean* (contains only the information about the properties of the system, but not of the laser pulse) power spectrum has been computed. To move system out of the equilibrium we used as an initial configuration the eigenstates of the HF Hamiltonian at elevated temperature ($T = 0.005$ a.u.). We propagate this solution during very long time interval (several ps) to get fine resolution for the spectra. A different number of basis functions and electrons has been included in the active space in order to understand its role on the formation of the plasmon peak (Fig. 6). Comparing this with the calculations with a larger basis set (Fig. 5), shows that only a small number of basis functions ($N_{bf} \sim 15$–25) is needed to get the correct position of the plasmon. However the fine details of the spectrum are quite sensitive to the size of active space. Another important feature of the *clean* spectra is the presence of the peaks at 1–2 eV, not available for the case, when the system is excited by laser pulse, which shows that some transitions might be forbidden for the particular polarization of the light, and can be excited only thermally.

4 Discussion and outlook

We developed a new computational scheme for the investigation of the electron dynamics in clusters under the influence of the external laser field within mean-field approximation. The solution of the TDHF equation was performed using the restricted Hartree-Fock functional for the closed shell systems, an expansion in Gaussian-type basis functions and employing effective core potential for the inner electrons.

The application of the TDHF method to the Na_9^+ cluster, previously intensively studied theoretically with different methods, and the Pt_3 cluster already accessible in the experimental investigation revealed the following capability of our approach: (i) the method is able to accurately predict the position of the plasmon peak for the Na_9^+ cluster, although its oscillator strength differs considerably from the TDLDA result. Two reasons for this difference could be suggested: different excitation mechanisms and the absence of an all-electron treatment in our case. Plasmon oscillations are a collective effect, that is why it is quite natural that a correct description of this phenomenon is only possible within the all-electron treatment. (ii) The calculation on the open-shell transition metal cluster Pt_3 allowed us not only to determine the position of the plasmon resonance, but also to estimate its lifetime by means of fitting the power spectra to a set of Lorentzians. Our value for the decay constant supports experimental evidence in favor of a bulk-like lifetime of the electronic excitations in this cluster.

Although our method is not able to embrace the whole variety of clusters and excitation regimes accessible experimentally we hope that it will become a useful theoretical tool in the investigation of nanoscale objects (up to several tens of atoms), where quantum effects are strong enough and the semiclassical approach, which is justified for larger systems, is not applicable any more.

This work was supported by the Deutsche Forschungsgemeinschaft through SFB 418.

References

1. H. Petek, S. Ogawa, Progr. Surf. Sci. **56**, 239 (1997)
2. T. Hertel, E. Knoesel, M. Wolf, G. Ertl, Phys. Rev. Lett. **76**, 535 (1996)
3. J.C. Diels, W. Rudolph, *Ultrashort Laser Pulse Phenomena* (Academic Press Inc., 1996)
4. A.P. Heberle, J.J. Baumberg, K. Köhler, Phys. Rev. Lett. **75**, 2598 (1996)
5. W.S. Warren, H. Rabitz, M. Dahleh, Science **259**, 1581 (1993)
6. M.S. Pshenichnikov, W.P. de Boeij, D.A. Wiersma, Phys. Rev. Lett. **76**, 4701 (1996)
7. D. Steinbach, G. Kocherscheidt, M.U. Wehner, H. Kalt, M. Wegener, K. Ohkawa, D. Hommel, V.M. Axt, Phys. Rev. B **60**, 12079 (1999)
8. J. Stenger, D. Madsen, P. Hamm, E.T.J. Nibbering, T. Elsaesser, Phys. Rev. Lett. **87**, 027401 (2001)
9. J.-Y. Bigot, V. Halte, J.-C. Merle, A. Daunois, Chem. Phys. **251**, 181 (2000)

10. V. Halte, J. Guille, J.-C. Merle, I. Perakis, J.-Y. Bigot, Phys. Rev. B **60**, 11738 (1999)
11. N. Pontius, P.S. Bechthold, M. Neeb, W. Eberhardt, Phys. Rev. Lett. **84**, 1132 (2000)
12. N.-H. Kwong, M. Bonitz, Phys. Rev. Lett. **84**, 1768 (2000)
13. M. Bonitz, J. W. Dufty, Chang Sub Kim, Phys. Stat. Sol. (b) **206**, 181 (1998)
14. P.A.M. Dirac, Proc. Camb. Philos. Soc. **26**, 376 (1930)
15. E. Runge, E.K.U. Gross, Phys. Rev. Lett. **52**, 997 (1984)
16. S.J.A. van Gisbergen, F. Kootstra, P.R.T. Schipper, O.V. Gritsenko, J.G. Snijders, E.J. Baerends, Phys. Rev. A **57**, 2556 (1998)
17. M. Madjet, C. Guet, W.R. Johnson, Phys. Rev. A **51**, 1327 (1995)
18. W. Ekardt, Phys. Rev. Lett. **52**, 1925 (1984)
19. K. Yabana, G.F. Bertsch, Phys. Rev. **54**, 4484 (1996)
20. The description of the free-electron final states requires the use of a delocalized basis set
21. *Gaussian 98*, Revision A.7, M.J. Frisch, G.W. Trucks, H.B. Schlegel, G.E. Scuseria, M.A. Robb, J.R. Cheeseman, V.G. Zakrzewski, J.A. Montgomery Jr, R.E. Stratmann, J.C. Burant, S. Dapprich, J.M. Millam, A.D. Daniels, K.N. Kudin, M.C. Strain, O. Farkas, J. Tomasi, V. Barone, M. Cossi, R. Cammi, B. Mennucci, C. Pomelli, C. Adamo, S. Clifford, J. Ochterski, G.A. Petersson, P.Y. Ayala, Q. Cui, K. Morokuma, D.K. Malick, A.D. Rabuck, K. Raghavachari, J.B. Foresman, J. Cioslowski, J.V. Ortiz, A.G. Baboul, B.B. Stefanov, G. Liu, A. Liashenko, P. Piskorz, I. Komaromi, R. Gomperts, R.L. Martin, D.J. Fox, T. Keith, M.A. Al-Laham, C.Y. Peng, A. Nanayakkara, C. Gonzalez, M. Challacombe, P.M.W. Gill, B. Johnson, W. Chen, M.W. Wong, J.L. Andres, C. Gonzalez, M. Head-Gordon, E.S. Replogle, J.A. Pople, Gaussian, Inc., Pittsburgh PA, 1998
22. F. Calvayrac, P.G. Reinhard, E. Suraud, Ann. Phys. (NY) **255**, 125 (1997)
23. W.H. Press, S.A. Teukolsky, W.T Vetteling, B.P. Flannery, *Numerical Recipes in Fortran 77 the Art of Scientific Computing*
24. R.C. Raffenetti, Chem. Phys. Lett. **20**, 335 (1973)
25. T.H. Dunning Jr, P.J. Hay, in *Modern Theoretical Chemistry*, edited H.F. Schaefer III (Plenum, New York, 1976)
26. P.J. Hay, W.R. Wadt, J. Chem. Phys. **82**, 284 (1985)
27. M. Brack, Rev. Mod. Phys. **65**, 677 (1993)
28. L. Hedin, S. Lundqvist, Solid State Phys. **23** (1969)
29. M. Bonitz, *Quantum kinetic theory* (Stuttgart, Teubner, 1998).
30. C.A. Ullrich, G. Vignale, Phys. Rev. Lett. **87**, 037402 (2001)
31. T. Dittrich, P. Hänggi, G.-L. Ingold, B. Kramer, G. Schön, W. Zwerger, in *Quantum transport and dissipation* (Wiley-VCH, Weinheim, 1998), Chap. 5
32. I.I. Rabi, Phys. Rev. **51**, 652 (1937)
33. E. Gilio, P.-G. Reinhard, E. Suraud, Comput. Mat. Sci. **17**, 534 (2000)
34. E. Gilio, P.G. Reinhard, E. Suraud, J. Phys. B: At. Mol. Opt. Phys. **33**, L333 (2000)
35. L. Féret, E. Suraud, F. Calvayrac, P.G. Reinhard, J. Phys. B: At. Mol. Opt. Phys. **29**, 4477 (1996)
36. F. Calvayrac, P.G. Reinhard, F. Suraud, Phys. Rev. B **52**, R17056 (1995)
37. H. Wang, E.A. Carter, J. Phys. Chem. **96**, 1197 (1992)
38. D.J. Rowe, *Nuclear Collective Motion* (Methuel, London, 1968)
39. B. Montag, P.-G. Reinhard, Phys. Rev. B **51**, 14686 (1995)
40. R.A. Molina, D. Weinmann, R.A. Jalabert, Phys. Rev. B **65**, 155427 (2002)